Gas-Phase Identity S_N2 Reactions of Halide Ions at Neutral Nitrogen: A High-Level Computational Study

Mikhail N. Glukhovtsev,[1a,b] Addy Pross,*[,1a,c] and Leo Radom*[,1d]

Contribution from the School of Chemistry, University of Sydney, Sydney, NSW 2006, Australia, Ben Gurion University of the Negev, Beer Sheva 84105, Israel, and Research School of Chemistry, Australian National University, Canberra, ACT 0200, Australia

Received February 9, 1995[⊗]

Abstract: High-level ab initio molecular orbital calculations at the G2(+) level of theory have been carried out for the identity nucleophilic substitution reactions at saturated nitrogen, $X^- + NH_2X \rightarrow XNH_2 + X^-$, for X = F, Cl, Br, and I, and the results compared with data for the analogous reactions at saturated carbon, $X^- + CH_3X \rightarrow XCH_3 + X^-$. Central barriers $\Delta H^{\ddagger}_{cent}$ for substitution at nitrogen are found to lie within a relatively narrow range, decreasing in the following order: Cl (58.5 kJ mol^{-1}) ≥ F (58.2 kJ mol^{-1}) > Br (46.9 kJ mol^{-1}) > I (39.1 kJ mol^{-1}). They are surprisingly similar to those for substitution at carbon, the barriers at nitrogen being slightly higher than the corresponding barriers at carbon for X = F and Cl and slightly lower for X = Br and I. The overall barriers relative to the reactants ($\Delta H^{\ddagger}_{ovr}$) are negative for all halogens: −55.8 (F), −9.3 (Cl), −13.7 (Br), and −10.9 kJ mol^{-1} (I), in contrast to the analogous reactions at carbon where the overall barrier is negative only for X = F. This suggests that nucleophilic substitution is likely to be more facile at nitrogen than at carbon. Stabilization energies of the ion−molecule complexes (ΔH_{comp}) decrease in the order F (114.0 kJ mol^{-1}) > Cl (67.8 kJ mol^{-1}) > Br (58.4 kJ mol^{-1}) > I (50.0 kJ mol^{-1}) and are found to correlate well with halogen electronegativities.

Introduction

The factors that govern barrier heights in simple gas-phase S_N2 identity exchange reactions remain poorly understood due, at least in part, to the difficulty in obtaining reliable theoretical and experimental energy data for these processes. In order to address this difficulty, we recently investigated the gas-phase energy profiles for the halide identity exchange reactions

$$X^- + CH_3X \rightarrow XCH_3 + X^- \quad (X = F, Cl, Br, \text{and } I) \quad (1)$$

as the G2(+) level of theory and found that the barrier heights for the set of halogens were clustered in a relatively small energy range (13.0 kJ mol^{-1} for the central barrier, $\Delta H^{\ddagger}_{cent}$).[2] Given the large differences in the bonding characteristics of the halogens (for example, the C−X bond strengths in CH_3X vary[3] between 230 and 465 kJ mol^{-1}), the small reactivity range was surprising. Furthermore, the barrier heights did not follow periodic ordering, but decreased in the order Cl > F ≥ Br > I.

In order to investigate the generality of this and other results, we embarked on a high-level study of the corresponding identity exchange reaction at nitrogen:

$$X^- + NH_2X \rightarrow XNH_2 + X^- \quad (X = F, Cl, Br, \text{and } I) \quad (2)$$

and the results are reported in the present paper. Nucleophilic substitution at a formally neutral saturated nitrogen has recently become the focus of increasing attention, both experimental[4−7] and theoretical,[8−10] so a comparison of the halide reactivity pattern at carbon with that at nitrogen is of interest. The detailed study of Bühl and Schaefer[9] is specially pertinent to the present work. We were particularly interested in establishing whether the prediction[2] of similar barriers for the range of halide exchange reactions at carbon also holds for the reactions at nitrogen or whether this pattern is specific to carbon. In addition, we wished to examine whether the prediction[9] that barriers for nucleophilic substitution at nitrogen are generally greater than those at carbon is confirmed by higher level calculations. Finally, we note that substitution at nitrogen is also of interest in relation to the carcinogenic properties of aromatic amines.[5,11]

Computational Methods

It is clear from the very large number of calculations already carried out on S_N2 reactions at carbon[2,12] that the computational data are very sensitive to the level of theory employed. For this reason, in our earlier study of S_N2 halide exchange at carbon,[2] we used a high level of theory, specifically a modification of G2 theory,[13] which appeared to be able to reproduce quite well the experimentally available data. In the present study, we apply this same level of theory to the nucleophilic substitution reactions at nitrogen.

⊗ Abstract published in *Advance ACS Abstracts,* August 1, 1995.

(1) (a) University of Sydney. (b) Permanent address: Institute of Physical and Organic Chemistry, Rostov University, 194/3 Stachka Ave., Rostov on Don, 344104, Russian Federation. (c) Ben-Gurion University of the Negev. (d) Australian National University.

(2) Glukhovtsev, M. N.; Pross, A.; Radom, L. *J. Am. Chem. Soc.* **1995**, *117*, 2024.

(3) Lias, S. G.; Bartmess, J. E.; Liebman, J. F.; Holmes, J. L.; Levin, R. D.; Mallard, W. G. *J. Phys. Chem. Ref. Data* **1988**, *17*, Suppl. 1.

(4) Erdik, E.; Ay, M. *Chem. Rev.* **1989**, *89*, 2796.

(5) (a) Ulbrich, R.; Famulok, M.; Bosold, F.; Boche, G. *Tetrahedron Lett.* **1990**, *31*, 1689. (b) Famulok, M.; Boche, G. *Angew. Chem., Int. Ed. Engl.* **1989**, *28*, 468.

(6) Helmick, J. S.; Martin, K. A.; Heinrich, J. L.; Novak, M. *J. Am. Chem. Soc.* **1991**, *113*, 3459. (b) Novak, M.; Martin, K. A.; Heinrich, J. L. *J. Org. Chem.* **1989**, *54*, 5430.

(7) Beak, P.; Li, J. *J. Am. Chem. Soc.* **1991**, *113*, 2796.

(8) Minkin, V. I.; Simkin, B. Y.; Minyaev, R. M. *Quantum Chemistry of Organic Compounds—Mechanisms of Reactions*; Springer-Verlag: Berlin, 1990; Chapter 5.

(9) (a) Bühl, M.; Schaefer, H. F. *J. Am. Chem. Soc.* **1993**, *115*, 364. (b) Bühl, M.; Schaefer, H. F. *J. Am. Chem. Soc.* **1993**, *115*, 9143.

(10) (a) Minyaev, R. M.; Wales, D. J. *J. Phys. Chem.* **1994**, *98*, 7942. (b) Minyaev, R. M. *Russ. Chem. Rev. (Engl. Transl.)* **1994**, *63*, 883.

0002-7863/95/1517-9012$09.00/0 © 1995 American Chemical Society

Standard ab initio molecular orbital calculations[14] were carried out using a modified form of G2 theory[13] with the GAUSSIAN-92 system of programs.[15] G2 theory corresponds effectively to calculations at the QCISD(T)/6-311+G(3df,2p) level with zero-point vibrational energy (ZPE) and higher level corrections. It has been shown[13,16,17] to perform well for the calculation of atomization energies, ionization energies, electron affinities, bond energies, proton affinities, acidities, and reaction barriers.

Our modifications to G2 theory have been introduced to allow a better description of anions and for computational simplification. In the first place, geometries were optimized and vibrational frequencies determined with a basis set that includes diffuse functions, specifically 6-31+G(d) in place of 6-31G(d) for first- and second-row atoms. In addition, the MP2/6-31+G(d) optimizations were carried out with the frozen-core approximation rather than with all electrons being included in the correlation treatment. Finally, harmonic vibrational frequencies were calculated at the HF/6-31+G(d) level rather than HF/6-31G(d). This level of theory is termed G2(+).

For bromine- and iodine-containing species, calculations were carried out with the use of basis sets incorporating the effective core potentials (ECPs) developed by Hay and Wadt.[18] The basis sets required for this so-called G2(+)[ECP] procedure are described in detail elsewhere.[19]

Table 1. Calculated G2(+) Total Energies (hartrees) for Species Involved in the Identity Exchange Reaction of X^- with NH_2X[a]

species	energy
F^-	−99.760 69
NH_2F	−155.532 99
$F^-\cdots HNHF$ (**1a**)	−255.337 09
FNH_2F^- (**2a**)	−255.314 92
$F^-\cdots H(H)NF$ (**3a**)	−255.330 14
Cl^-	−459.808 99
NH_2Cl	−515.561 68
$Cl^-\cdots HNHCl$ (**1b**)	−975.396 50
$ClNH_2Cl^-$ (**2b**)	−975.374 22
$Cl^-\cdots H(H)NCl$ (**3b**)	−975.395 05
Br^-	−13.229 29
NH_2Br	−68.977 51
$Br^-\cdots HNHBr$ (**1c**)	−82.229 06
$BrNH_2Br^-$ (**2c**)	−82.212 02
$Br^-\cdots H(H)NBr$ (**3c**)	−82.228 36
I^-	−11.446 98
NH_2I	−67.197 78
$I^-\cdots NHNI$ (**1d**)	−78.663 79
INH_2I^- (**2d**)	−78.648 89
$I^-\cdots H(H)NI$ (**3d**)	−78.663 27

[a] Values listed are all-electron (AE) G2(+) energies for F- and Cl-containing species and effective-core-potential (ECP) G2(+) energies for Br- and I-containing species.

Geometries and harmonic vibrational frequencies were obtained through calculations that we refer loosely to overall (i.e. including Br and I) as MP2/6-31+G(d,p) or HF/6-31+G(d,p). Again, we refer loosely to the ultimate basis set used in our G2(+) calculations (i.e. again including the supplemented ECP basis sets for Br and I) as 6-311+G(3df,2p). Note that we have recommended[19] alternative ECP basis sets for bromine and iodine for use in *standard G2(ECP)* calculations.

Charge distributions were obtained from the wave functions calculated at the MP2/6-311+G(3df,2p) level on MP2/6-31+G(d) geometries, employing natural population analysis (NPA).[20,21]

Calculated total energies are presented in Table 1. Unless otherwise stated, we have used the results of all-electron (G2(+)[AE]) calculations for F- and Cl-containing molecules and effective-core-potential (G2(+)[ECP]) calculations for Br- and I-containing molecules in our analysis. Throughout this paper, bond lengths are in angstroms and bond angles are in degrees. All relative energies in this paper correspond to enthalpy changes (ΔH) at 0 K, as indicated; ΔE and ΔH are, of course, identical at 0 K.

Results and Discussion

The energy profile for gas-phase nucleophilic substitution at nitrogen is described by a double-well potential curve (Figure 1), analogous to that at carbon found computationally[22] and experimentally.[23] Thus, the reaction involves the initial forma-

(11) (a) Singer, B.; Kusmierek, J. T. *Annu. Rev. Biochem.* **1982**, *51*, 655. (b) Lai, C. C.; Miller, E. C.; Miller, J. A.; Leim, A. *Carcinogenesis* **1987**, *8*, 471. (c) Lai, C. C.; Miller, E. C.; Miller, J. A.; Liem, P. *Carcinogenesis* **1988**, *9*, 1295.

(12) Comprehensive collections of both experimental and computational data on S_N2 reactions at saturated carbon (up to 1991) may be found in the following monograph: (a) Shaik, S. S.; Schlegel, H. B.; Wolfe, S. *Theoretical Aspects of Physical Organic Chemistry, The S_N2 Mechanism*; Wiley: New York, 1992. See also: (b) Basilevsky, M. V.; Koldobskii, S. G.; Tikhomirov, V. A. *Russ. Chem. Rev. (Engl. Transl.)* **1986**, *55*, 948. For more recent references, see, for example: (c) Anh, N. T.; Maurel, F.; Thanh, B. T.; Thao, H. H.; N'Guessan, Y. T. *New J. Chem.* **1994**, *18*, 473. (d) Wladkowski, B. D.; Allen, W. D.; Brauman, J. I. *J. Phys. Chem.* **1994**, *98*, 13532 and references cited therein.

(13) Curtiss, L. A.; Raghavachari, K.; Trucks, G. W.; Pople, J. A. *J. Chem. Phys.* **1991**, *94*, 7221.

(14) Hehre, W. J.; Radom, L.; Schleyer, P. v. R.; Pople, J. A. *Ab Initio Molecular Orbital Theory*; Wiley: New York, 1986.

(15) Frisch, M. J.; Trucks, G. W.; Head-Gordon, M.; Gill, P. M. W.; Wong, M. W.; Foresman, J. B.; Johnson, B. G.; Schlegel, H. B.; Robb, M. A.; Replogle, E. S.; Gomperts, R.; Andres, J. L.; Raghavachari, K.; Binkley, J. S.; Gonzalez, C.; Martin, R. L.; Fox, D. J.; DeFrees, D. J.; Baker, J.; Stewart, J. J. P.; Pople, J. A. GAUSSIAN-92; Gaussian Inc.: Pittsburgh, PA, 1992.

(16) See, for example: (a) Curtiss, L. A.; Koch, D.; Pople, J. A. *J. Chem. Phys.* **1991**, *95*, 4040. (b) Curtiss, L. A.; Raghavachari, K.; Deutsch, P. W.; Pople, J. A. *J. Chem. Phys.* **1991**, *95*, 2433. (c) Pople, J. A.; Curtiss, L. A. *J. Chem. Phys.* **1991**, *95*, 4385. (d) Curtiss, L. A.; Nobes, R. H.; Pople, J. A.; Radom, L. *J. Chem. Phys.* **1992**, *97*, 6766. (e) Curtiss, L. A.; Raghavachari, K.; Pople, J. A. *Chem. Phys. Lett.* **1993**, *214*, 183. For recent reviews, see: (f) Curtiss, L. A.; Raghavachari, K. In *Quantum Mechanical Electronic Structure Calculations with Chemical Accuracy*; Langhoff, S. R., Ed.; Kluwer Academic Press: The Netherlands, 1995. (g) Raghavachari, K.; Curtiss, L. A. In *Modern Electronic Structure Theory*; Yarkony, D. R., Ed.; World Scientific: Singapore, 1995.

(17) See, for example: (a) Smith, B. J.; Radom, L. *J. Phys. Chem.* **1991**, *95*, 10549. (b) Ma, N. L.; Smith, B. J.; Pople, J. A.; Radom, L. *J. Am. Chem. Soc.* **1991**, *113*, 7903. (c) Smith, B. J.; Curtiss, L. A.; Pople, J. A.; Radom, L. *Aust. J. Chem.* **1992**, *45*, 285. (d) Nobes, R. H.; Radom, L. *Chem. Phys. Lett.* **1992**, *189*, 554. (e) Yu, D.; Rauk, A.; Armstrong, D. A. *J. Phys. Chem.* **1992**, *96*, 6031. (f) Wong, M. W.; Radom, L. *J. Am. Chem. Soc.* **1993**, *115*, 1507. (g) Smith, B. J.; Radom, L. *J. Am. Chem. Soc.* **1993**, *115*, 4885. (h) Schlegel, H. B.; Skancke, A. *J. Am. Chem. Soc.* **1993**, *115*, 7465. (i) Goldberg, N.; Hrusák, J.; Iraqi, M.; Schwarz, H. *J. Phys. Chem.* **1993**, *97*, 10687. (j) Armstrong, D. A.; Rauk, A.; Yu, D. *J. Am. Chem. Soc.* **1993**, *115*, 666. (k) Wiberg, K.; Rablen, P. R. *J. Am. Chem. Soc.* **1993**, *115*, 9234. (l) Wiberg, K.; Nakaji, D. *J. Am. Chem. Soc.* **1993**, *115*, 10658. (m) Lammertsma, K.; Prasad, B. V. *J. Am. Chem. Soc.* **1994**, *116*, 642. (n) Gauld, J. W.; Radom, L. *J. Phys. Chem.* **1994**, *98*, 777. (o) Chiu, S.-W.; Li, W.-K.; Tzeng, W.-B.; Ng, C.-Y. *J. Chem. Phys.* **1992**, *97*, 6557. (p) Durant, J. L.; Rohlfing, C. M. *J. Chem. Phys.* **1993**, *98*, 8031. (q) Glukhovtsev, M. N.; Pross, A.; Radom, L. *J. Am. Chem. Soc.* **1994**, *116*, 5961. (r) Glukhovtsev, M. N.; Szulejko, J. E.; McMahon, T. B.; Gauld, J. W.; Scott, A. P.; Smith, B. J.; Pross, A.; Radom, L. *J. Phys. Chem.* **1994**, *98*, 13099.

(18) Wadt, W. R.; Hay, P. J. *J. Chem. Phys.* **1985**, *82*, 284.

(19) Glukhovtsev, M. N.; Pross, A.; McGrath, M. P.; Radom, L. *J. Chem. Phys.* **1995**, in press.

(20) (a) Reed, A. R.; Weinstock, R. B.; Weinhold, F. *J. Chem. Phys.* **1985**, *83*, 735. (b) Reed, A. E.; Curtiss, L. A.; Weinhold, F. *Chem. Rev.* **1988**, *88*, 899. (c) Weinhold, F.; Carpenter, J. E. In *The Structure of Small Molecules and Ions*; Naaman, R., Vager, Z., Eds.; Plenum Press: New York, 1988; p 227. (d) Reed, A. E.; Weinhold, F. *Isr. J. Chem.* **1991**, *31*, 277. For recent NPA applications, see, e.g.: (e) Reed, A. E.; Schleyer, P. v. R. *J. Am. Chem. Soc.* **1990**, *112*, 1434. (f) Glukhovtsev, M. N.; Schleyer, P. v. R. *Chem. Phys. Lett.* **1992**, *198*, 547. (g) Mestres, J.; Duran, M.; Bertran, J. *Theor. Chim. Acta* **1994**, *88*, 325. (h) Nemukhin, A. V.; Grigorenko, B. L. *Chem. Phys. Lett.* **1995**, *233*, 627.

(21) Calculated NPA charges are available as supporting information (Tables S1−S3).

(22) (a) Dedieu, A.; Veillard, A. *Chem. Phys. Lett.* **1970**, *5*, 328. (b) Dedieu, A.; Veillard, A. *J. Am. Chem. Soc.* **1972**, *94*, 6730.

(23) (a) Olmstead, W. N.; Brauman, J. I. *J. Am. Chem. Soc.* **1977**, *99*, 4219. (b) Pellerite, M. J.; Brauman, J. I. *J. Am. Chem. Soc.* **1980**, *102*, 5993. (c) Pellerite, M. J.; Brauman, J. I. *J. Am. Chem. Soc.* **1983**, *105*, 2672. (d) Pellerite, M. J.; Brauman, J. I. In *Mechanistic Aspects of Inorganic Reactions*; Rorabacher, D. R., Endicott, J. F., Eds.; ACS Symposium Series; American Chemical Society: Washington, DC, 1982; Vol. 198, p 81. (e) Riveros, J. M.; Jose, S. M.; Takashima, K. *Adv. Phys. Org. Chem.* **1985**, *21*, 197.

Table 2. Geometrical Parameters for NH_2X (X = F, Cl, Br, and I)[a]

species	level[b]	r(N−X)	r(N−H)	∠XNH	∠HNH
NH_2F	MP2/6-31+G(d)	1.446	1.024	100.6	106.0
	expt[c]	1.436	1.027	100.9	105.5
NH_2Cl	MP2/6-31+G(d)	1.752	1.022	105.2	106.6
	expt[d]	1.748	1.017	103.7	107.4
NH_2Br	MP2/6-31+G(d)−ECP	1.920	1.023	104.2	106.5
NH_2I	MP2/6-31+G(d)−ECP	2.083	1.024	105.4	106.5

[a] Bond lengths in angstroms, bond angles in degrees. [b] See text for details of the Br and I basis sets. [c] From ref 27, r_z-structure. [d] From ref 28.

tion of a reactant ion−molecule complex, **1**, with a complexation energy, ΔH_{comp}, relative to separated reactants. This complex must then overcome an activation barrier that we term the *central* barrier, $\Delta H^{\ddagger}_{cent}$, to reach a transition structure, **2**,which

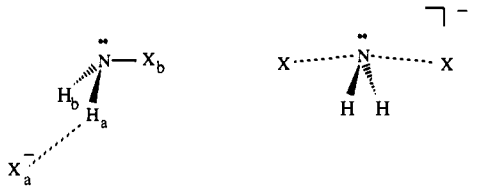

1 (C_1) **2** (C_{2v})

(**a**: X = F, **b**: X = Cl, **c**: X = Br, **d**: X = I)

then breaks down to give the product ion−molecule complex, **1′**.[24] Finally, the product ion−molecule complex dissociates into separated products. The *overall* activation barrier relative to separated reactants (rather than to the complex) is denoted $\Delta H^{\ddagger}_{ovr}$. For the set of identity reactions described here, reactants and products are of course identical, as are the reactant ion−molecule and product ion−molecule complexes.

A. NH_2X Structures (X = F, Cl, Br, and I). Calculated NH_2X geometries are compared with available experimental data[27,28] in Table 2 and show good agreement for the experimentally characterized NH_2F and NH_2Cl molecules. Calculated charge distributions[21] show that the fluorine atom in NH_2F bears a negative charge, in contrast to the results for the other NH_2X molecules where the chlorine, bromine, and iodine atoms are found to bear a positive charge. While charges on the hydrogens change little from NH_2F to NH_2I, the negative charge on nitrogen increases considerably from NH_2F to NH_2I.[21]

B. Ion−Molecule Complexes. Approach of X^- to NH_2X can lead to the formation of different ion−molecule complexes, $X^-\cdots NH_2X$, depending on whether the halide ion coordinates with just one hydrogen as in **1**, with two hydrogens as in **3**, or with the halogen atom of the NH_2X molecule as in **4**. In

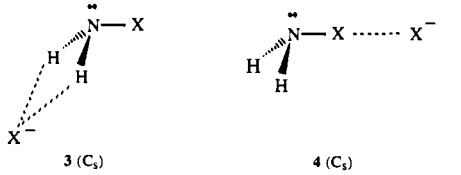

3 (C_s) **4** (C_s)

accordance with the recent computational study of reaction 2 for X = F and Cl by Bühl and Schaefer,[9] we have found that the preferred structures for all $X^-\cdots NH_2X$ (X = F−I) ion−molecule complexes are of type **1** with C_1 symmetry (Table 3). Structures of the type **3** are found to be transition structures in the halide anion migration between the two hydrogens in **1** (Table 4).

Structure **4** would correspond to a pre-reaction complex in the so-called halophilic substitution pathway.[29] Since calculations for X = F showed[9b] the halophilic pathway to be highly endothermic,[30] it is not considered further in this work. Proton−transfer reactions, which may also compete with nucleophilic substitution,[9b] were also not considered.

1. Complexation Energies. G2(+) complexation energies (ΔH_{comp}, see Figure 1) for **1a−1d** are presented in Table 5 together with corresponding values for complexes, $X^-\cdots CH_3X$.

Our calculated complexation energies for X = F (114.0 kJ mol^{-1}) and Cl (67.8 kJ mol^{-1}) are slightly greater than those obtained by Bühl and Schaefer[9] (110.6 kJ mol^{-1} for X = F at CISD/TZP+ plus ZPVE and 55.2 kJ mol^{-1} for X = Cl at HF/DZP+ plus ZPVE).[31] Experimental data for $X^-\cdots HNHX$ (X = F−I) complexation energies are not available. However, our G2(+) complexation energy for $F^-\cdots HNHF$ (114.0 kJ mol^{-1}) is close to that for the F···HNHPh complex (112.1 kJ mol^{-1}).[33]

The G2(+) complexation energies for $X^-\cdots HNHX$ (X = F, Cl, Br, and I), **1a−1d**, are found to decrease in the order F > Cl > Br > I and show a good linear correlation with halogen electronegativities using the Mulliken (R^2 = 0.975), Pauling (R^2 = 0.985), or Allred−Rochow (R^2 = 0.977) electronegativity scales.[34] The correlation with the Mulliken scale is shown in Figure 2. We find similarly good correlations between the complexation energies and the absolute electronegativities[35] as well as the absolute hardness[35] of the halide anions (R^2 = 0.974 and 0.999, respectively). These correlations for the $X^-\cdots HNHX$ complexes are analogous to those found for $X^-\cdots CH_3X$ complexes,[2] although the complexation energies are larger for $X^-\cdots HNHX$ than for the corresponding carbon complexes (Table 5, Figure 3). The larger complexation energies for $X^-\cdots HNHX$ compared with $X^-\cdots CH_3X$ are consistent with the N−H bond being an effective proton donor, leading to significant X···H−N hydrogen bonding in the $X^-\cdots HNHX$ complexes.

Activation barriers for the halide anion migrations in **1** via **3** are also given in Table 5. For X = F, the barrier of 18.2 kJ mol^{-1} (close to the barrier of 19.2 kJ mol^{-1} found at the CISD/TZP+ plus ZPVE level by Bühl and Schaefer[9a]) is considerably larger than that for X = Cl−I. Activation barriers in the X^- anion migration for X = Cl−I decrease from 3.8 (X = Cl) to 1.4 kJ mol^{-1} (X = I) and imply that the complexes **1b−1d** have rather flexible structures. The large differences between

(24) Minyaev and Wales[10] have pointed out that in a strict mathematical sense the steepest descent pathway from transition structure **2** proceeds past a valley ridge inflection point to the transition structure **3** for halide ion exchange.[25,26] In practice, the system is unlikely to stay on the ridge and will collapse directly to the ion−molecule complex **1**. An analysis of the dynamics of this system, particularly near the valley-ridge inflection point, would give valuable insight into this complex reaction.

(25) Valtazanos, P.; Ruedenberg, K. *Theor. Chim. Acta* **1986**, *69*, 281.
(26) Schlegel, H. B. *J. Chem. Soc., Faraday Trans.* **1994**, *90*, 1569.
(27) Christen, D.; Minkwitz, R.; Nass, R. *J. Am. Chem. Soc.* **1987**, *109*, 7020.
(28) Harmony, M. D.; Laurie, V. W.; Kuczkowski, R. L.; Schwendeman, R. H.; Ramsay, D. A.; Lovas, F. J.; Lafferty, W. J.; Maki, A. G. *J. Phys. Chem. Ref. Data* **1979**, *8*, 619.
(29) Zefirov, N. S.; Makhon'kov, D. I. *Chem. Rev.* **1982**, *82*, 615.
(30) At HF/DZP+, the enthalpy change for the reaction $NH_2F + F^- \rightarrow NH_2^- + F_2$ was calculated[9b] to be 485.3 kJ mol^{-1}.
(31) The HF/DZP+ complexation energy for X = Cl is not given directly in ref 9b but was calculated from the data presented in Table 1 of ref 9b with the use of HF/DZP zero-point energies[9b] scaled by 0.9135.[32]
(32) Pople, J. A.; Scott, A. P.; Wong, M. W.; Radom, L. *Isr. J. Chem.* **1993**, *33*, 345.
(33) Larson, J. W.; McMahon, T. B. *J. Am. Chem. Soc.* **1983**, *105*, 2944.
(34) For a discussion of the current status of the electronegativity concept in chemistry and for leading references, see: (a) Allen, L. C. *Int. J. Quantum Chem.* **1994**, *49*, 253. (b) Allen, L. C. *J. Am. Chem. Soc.* **1989**, *111*, 9003. (c) Bratsch, S. G. *J. Chem. Educ.* **1988**, *65*, 34. (d) Meek, T. L. *J. Chem. Educ.* **1993**, *70*, 799.
(35) Pearson, R. G. In *The Concept of Chemical Bonding*; Maksic, Z. B., Ed.; Springer-Verlag: Berlin, 1990; p 45.

Table 3. Geometrical Parameters for Ion−Molecule Complexes $X^-\cdots HNHX$ (**1**, X = F, Cl, Br, and I) and Relative Elongations of the N−H_a Bond Lengths (% N−H_a) due to Complexation[a−c]

species	$r(X_a\cdots H_a)$	$r(N-X_b)$	$r(N-H_a)$	$r(N-H_b)$	$\angle X_aH_aN$	$\angle H_aNH_b$	$\angle H_aNX_b$	$\angle H_bNX_b$	$\angle X_aH_aH_bN$	% N−H_a[d]
1a (X = F)	1.554	1.477	1.075	1.025	166.0	102.8	103.1	98.8	168.7	5.0
1b (X = Cl)	2.215	1.762	1.040	1.023	161.9	103.2	105.7	103.6	172.3	1.8
1c (X = Br)	2.428	1.926	1.039	1.025	156.5	102.8	104.8	102.8	169.5	1.5
1d (X = I)	2.669	2.085	1.037	1.026	156.0	103.4	105.5	104.1	171.7	1.3

[a] Bond lengths in angstroms, bond angles in degrees. [b] MP2/6-31+G(d) level. See text for details of the Br and I basis sets. [c] Bond lengths and angles refer to those indicated in structure **1**. [d] Defined by eq 3.

Table 4. Geometrical Parameters for Transition Structures $X^-\cdots H_2NH$ (**3**, X = F, Cl, Br, and I)[a−c]

species	$r(X_a\cdots H)$	$r(N-X_b)$	$r(N-H)$	∠HNH	$\angle X_aHHN$[d]	$\angle X_bN(HH)$[e]
3a (X = F)	1.961	1.477	1.027	96.2	158.6	107.5
3b (X = Cl)	2.648	1.765	1.025	99.7	166.3	113.9
3c (X = Br)	2.811	1.930	1.027	100.5	163.9	112.6
3d (X = I)	3.043	2.088	1.028	101.3	166.1	114.3

[a] Bond lengths in angstroms, bond angles in degrees. [b] MP2/6-31+G(d) level. See text for details of the Br and I basis sets. [c] X_a is the incoming halide anion while X_b is the halogen atom in the NH_2X moiety in **3**. [d] Angle between X_aHH and HHN planes. [e] Angle between N−X_b bond and NHH plane.

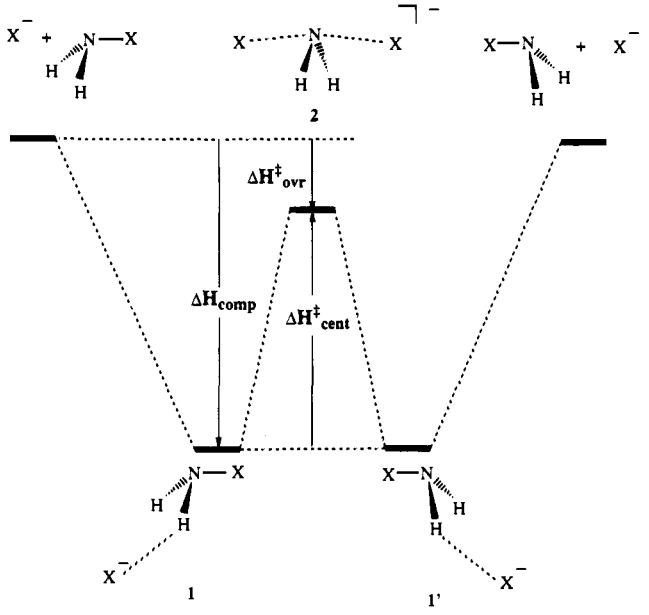

Figure 1. Schematic energy profile for the X^- + NH_2X identity exchange reaction (X = F−I).

Table 5. Complexation Energies (ΔH_{comp}) of the Ion−Molecule Complexes, Overall Barrier Heights Relative to Reactants ($\Delta H^{\ddagger}_{ovr}$), and Central Barriers ($\Delta H^{\ddagger}_{cent}$) for X^- + NH_2X Reactions, as well as Barriers for the Halide Anion Migration in **1** (G2(+), kJ mol^{-1})[a]

X	ΔH_{comp}[b]	$\Delta H^{\ddagger}_{ovr}$[b]	$\Delta H^{\ddagger}_{cent}$[b]	$\Delta H^{\ddagger}$[c]
F	114.0 (56.5)	−55.8 (−8.0)	58.2 (48.5)[d]	18.2
Cl	67.8 (44.0)	−9.3 (11.5)	58.5 (55.5)	3.8
Br	58.4 (41.1)	−13.7 (5.8)	44.7 (46.9)	1.8
I	50.0 (36.0)	−10.8 (6.5)	39.1 (42.5)	1.4

[a] See Figure 1 for definition of energy quantities. [b] Values in parentheses are corresponding energies for X^- + CH_3X reactions 1, taken from ref 2. [c] Barrier for X^- migration in **1** via **3**. [d] The G2(+) central barrier for reaction 1 with X = F (48.5 kJ mol^{-1}) is close to the barrier height (53.6 ± 6.3 kJ mol^{-1}) obtained by extrapolation from CCSD(T) calculations using a [13s8p6d4f,8s6p4d] basis set.[12d]

the activation barrier for X = F and those for X = Cl−I presumably reflect the relative magnitudes of the corresponding complexation energies and H···X bond lengths.

2. Geometries. The calculated geometries of complexes **1a−1d** and transition structures **3a−3d** are presented in Tables 3 and 4, respectively. The geometries of the NH_2X moieties

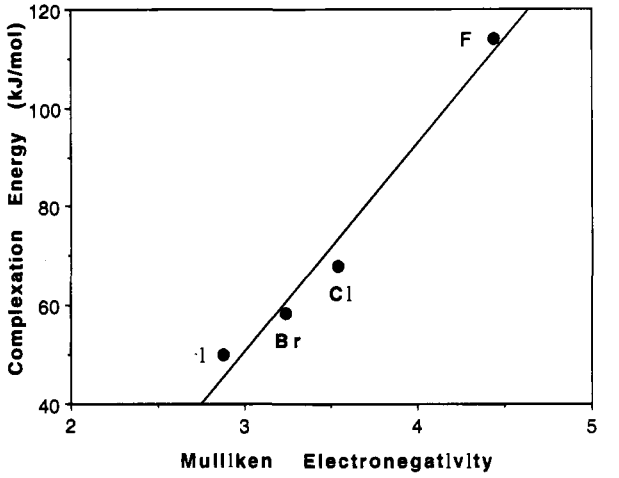

Figure 2. Plot of G2(+) complexation energies (ΔH_{comp}) of the ion−molecule complexes **1** vs Mulliken electronegativities (in Pauling units, taken from ref 34b) of the halogens. ΔH_{comp} values are listed in Table 5.

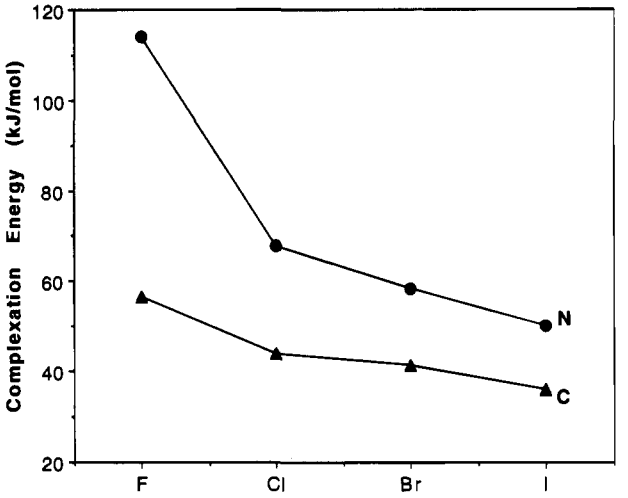

Figure 3. Comparison of G2(+) complexation energies (ΔH_{comp}) of the ion−molecule complexes X^-···HNHX (●) and X^-···H_3CX (▲) for X = F−I.

in the X^-···H_2NX species, **1** and **3**, differ only slightly from those in the unperturbed NH_2X molecules (Table 2). For **1**, the main changes are found in the N−H_a bond length, which is slightly elongated in the complex. Values of the extent of elongation, defined by % N−H_a

$$\%\ N-H_a = 100(d^{comp}{}_{N-H} - d^{react}{}_{N-H})/d^{react}{}_{N-H} \quad (3)$$

(where $d^{comp}{}_{N-H}$ and $d^{react}{}_{N-H}$ are the N−H_a bond length in the ion−molecule complex **1** and the N−H bond length in the reactant NH_2X molecule, respectively), are listed in Table 3 and are found to correlate with the corresponding complexation energies (R^2 = 0.981), i.e., the larger the complexation energy, the greater the N−H_a bond elongation in **1**. Accordingly, the largest % N−H_a value is found for the F^-···H_2NF complex.

Table 6. Geometries of the XNH_2X^- Transition Structures (**2**, X = F, Cl, Br, and I)[a,b]

species	r(X···N)	r(N−H)	∠XNX	∠HNH	% N−X‡ [c]
2a (X = F)	1.833	1.015	163.9	105.8	24.1 (26.2)
2b (X = Cl)	2.220	1.022	171.3	104.8	26.0 (28.0)
2c (X = Br)	2.357	1.026	174.0	104.4	22.4 (24.7)
2d (X = I)	2.506	1.031	178.8	103.9	20.2 (23.2)

[a] Bond lengths in angstroms, bond angles in degrees. [b] MP2/6-31+G(d) level. See text for details of the Br and I basis sets. [c] % N−X‡ is the MP2-calculated index of bond cleavage in transition structures **2** (see eq 4). The analogous % C−X‡ values for reaction 1 are shown in parentheses.

The N−H···X⁻ hydrogen bond should benefit from a linear arrangement.[36] Indeed, the N−H···X⁻ fragment in **1** is closer to a linear arrangement (cf. the $\angle X_aH_aN$ angle in Table 3) for those complexes with a larger complexation energy (Table 5).

3. Charge Distributions. Calculated charges in **1**[21] suggest that charge transfer from X⁻ to NH_2X, though relatively small, decreases from F to I and reflects the magnitude of the complexation energy, which decreases in the same order. Charges on the incoming halide anion X_a^- in the transition structures **3** are larger in absolute value than those in the complexes **1**, while the nitrogen correspondingly bears less negative charge in **3** than in **1**.[21]

C. Transition Structures and Barrier Heights. Only transition structure **2**, obtained from back-side attack at N, has been considered. The possibility of front-side attack, which was found to be associated with much higher barriers in the analogous reactions at carbon,[8,12b,37,38] is expected to be even less favored for attack at the more electronegative nitrogen.[12b,38] G2(+) values for the central barriers ($\Delta H^{\ddagger}_{cent}$) and the overall barriers relative to separated reactants ($\Delta H^{\ddagger}_{ovr}$) are included in Table 5. Geometries of the C_{2v} transition structures (**2**) are presented in Table 6.

1. Barriers. Calculated central barriers ($\Delta H^{\ddagger}_{cent}$) for the identity reaction $X^- + NH_2X$ (X = F, Cl, Br, and I) lie within a range of about 20 kJ mol⁻¹ (from 39.1 kJ mol⁻¹ for X = I up to 58.5 kJ mol⁻¹ for X = Cl). This result parallels that found for substitution at carbon for which there is also only a small variation in the central barriers (from 42.5 kJ mol⁻¹ for X = I to 55.5 kJ mol⁻¹ for X = Cl).[2] Of particular interest is the observation that the intrinsic reactivities of the two reaction families are very similar. For X = F and Cl the barriers for substitution at nitrogen are found to be slightly higher than those for substitution at carbon, while for X = Br and I the barriers are marginally lower (Table 5, Figure 4). Our results differ from earlier calculations at lower levels of theory (HF/DZP+, CISD/TZP+, and CCSD/DZP+ for X = F and HF/DZP+ for X = F, Cl, OH, CN, and H),[9] from which it was concluded that barriers for substitution are generally substantially larger at nitrogen than at carbon. At the lower MP2/6-311+G(d,p) + ZPVE (HF/6-31+G(d)) level, we also find that the barrier at nitrogen (84.4 kJ mol⁻¹) is significantly greater than the corresponding barrier at carbon (64.6 kJ mol⁻¹) for X = F. Indeed, the MP2/6-311+G(d,p) + ZPVE barrier for X = F (84.4 kJ mol⁻¹) is reasonably close to that reported at the CISD/TZP+ plus ZPVE level (97.3 kJ mol⁻¹) but significantly different from the G2(+) value of 58.2 kJ mol⁻¹. For X = Cl, the difference between the barriers at nitrogen and carbon, as calculated at the MP2/6-311+G(d,p) + ZPVE (HF/6-31+G(d)) level, is not very large (79.3 vs 73.4 kJ mol⁻¹), in this case consistent with the G2(+) results. Our results thus show that the variation with level of theory differs from system to system. They therefore reaffirm the importance of high levels of correlation and large basis sets in assessing both absolute *and* relative barrier heights in S_N2-type substitution reactions.

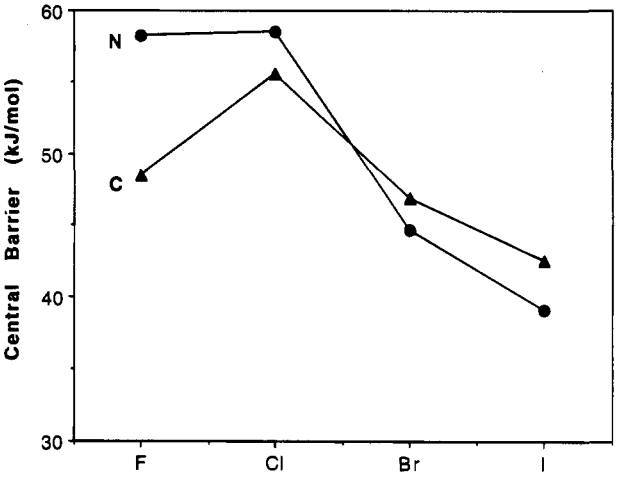

Figure 4. Comparison of G2(+) central barriers ($\Delta H^{\ddagger}_{cent}$) for the S_N2 identity reactions at nitrogen (●) and carbon (▲) for X = F−I. G2(+) $\Delta H^{\ddagger}_{cent}$ values are given in Table 5.

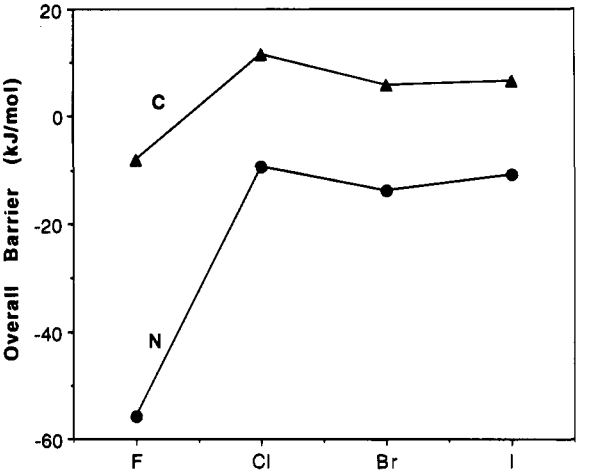

Figure 5. Comparison of G2(+) overall barriers ($\Delta H^{\ddagger}_{ovr}$) for the S_N2 identity reactions at nitrogen (●) and at carbon (▲) for X = F−I. G2(+) $\Delta H^{\ddagger}_{ovr}$ values are given in Table 5.

In our earlier paper on $X^- + CH_3X$, we attributed the similar barrier heights for different X (at least when X is restricted to the family of halogens) to the fact that the transition state involves the simultaneous making and breaking of the same bond. Thus, we found that despite the large difference in the C−X bond strengths for different X, and the large variation in the proton and methyl cation affinities of X⁻, the barriers for the identity exchange of halide at carbon end up being quite similar.[2] The fact that a similar reactivity pattern is also reproduced for $X^- + NH_2X$ strengthens this earlier assessment that barrier heights for halide exchange are not greatly influenced by the identity of the halogen, and it also suggests that the reactivity pattern for substitution at carbon and nitrogen is influenced more by properties of the halogen family than by the nature of the atom undergoing attack.

The G2(+) overall barriers ($\Delta H^{\ddagger}_{ovr}$) for $X^- + NH_2X$ are significantly lower than the corresponding values for carbon (Table 5 and Figure 5), although the barrier *patterns* are quite similar. For $X^- + NH_2X$, the overall barriers are all *negative* in contrast to the values for substitution at carbon which are positive for X = Cl, Br, and I (Figure 5).[2] The lower overall

(36) See, for example: Scheiner, S. *J. Mol. Struct. (Theochem)* **1994**, *307*, 65.

(37) Schlegel, H. B.; Mislow, K.; Bernardi, F.; Bottoni, A. *Theor. Chim. Acta* **1977**, *44*, 245.

(38) Anh, N. T.; Minot, C. *J. Am. Chem. Soc.* **1980**, *102*, 103.

barriers are consistent with the larger complexation energies for X^-···HNHX and the very similar central barriers for reaction at N and at C. Our results differ from earlier HF/DZP+ calculations[9b] which indicated positive overall barriers for substitution at nitrogen for X = F and Cl, while CISD/TZP+ plus ZPVE calculations[9a] for X = F showed a negative $\Delta H^{\ddagger}_{ovr}$ barrier of −13.4 kJ mol^{-1}, significantly less negative than our G2(+) value of −55.8 kJ mol^{-1} (Table 5). At the MP2/6-311+G(d,p) + ZPVE(HF/6-31+G(d)) level, we find the overall barriers to be −28.4 and +12.5 kJ mol^{-1} for X = F and Cl, respectively.

To the best of our knowledge, no experimental data for gas-phase nucleophilic substitution at nitrogen are available. Given that we find the overall barriers are negative, we would predict that gas-phase nucleophilic substitution reactions at neutral nitrogen are energetically facile. However, it is possible that other competitive processes, e.g. proton transfer, will be favored, so that the substitution pathway is not necessarily the one that would be experimentally observed.

2. Geometries. The N−H bond lengths in the C_{2v} transition structures **2a**−**2d** are found to be similar in magnitude, increasing marginally from 1.015 (**2a**) to 1.031 Å (**2d**) (Table 6). The C−H bond lengths in the D_{3h} transition structures for exchange at carbon behave similarly.[2] The ∠XNX angle is found to widen from 163.9° in **2a** to 178.8° in **2d** (Table 6).

The looseness of the C_{2v} XNH_2X^- transition structures **2** may be quantified by a looseness parameter (% N−X‡) in a way similar to that proposed for methyl-transfer reactions.[12a] Thus we may write

$$\% \text{ N}-\text{X}^{\ddagger} = 100(d^{\ddagger}_{\text{N}-\text{X}} - d^{\text{comp}}_{\text{N}-\text{X}})/d^{\text{comp}}_{\text{N}-\text{X}} \qquad (4)$$

where $d^{\ddagger}_{N-X}$ and d^{comp}_{N-X} are the N−X bond lengths in transition structure **2** and ion−molecule complex **1**, respectively. We find, as with the substitution reaction at carbon, that the % N−X‡ values for different X are close to one another and decrease in the order Cl > F > Br > I (Table 6).

3. Charge Distributions. Charge distributions in the transition structures XNH_2X^- reveal a substantial positive charge on the NH_2 moiety only for X = F.[21] This suggests a significant contribution of the triple-ion valence bond (VB) configuration, $F^-(NH_2)^+F^-$ in **2a**, similar to that found in the analogous reaction at carbon.[2] In view of the fact that overall barrier heights for X^- + NH_2X and X^- + CH_3X are lower for X = F than for the other halogens, it is possible that this added stabilization is due to the mixing in of the triple-ion configuration into the transition state wave function. For other halogens, particularly for X = I, the negative charge of the NH_2 moiety, as well as the smaller negative charge on the iodine atoms (less than 0.5 electron), suggests that the VB configuration $X\cdot(NH_2)^-\cdot X$ may override a reduced contribution of $X^-(NH_2)^+X^-$.[21]

D. Correlations of Central Barrier Heights. There has been considerable discussion in the literature as to what factors might influence barrier heights in gas-phase S_N2 reactions at saturated carbon.[12,23c,d] Recently we studied some of these factors using our data at the G2(+) level of theory.[2] In this section we discuss our computational data for substitution at nitrogen in the same context. Our main finding is that substitution at nitrogen shows similar patterns of behavior to substitution at carbon but with the overall barrier heights being significantly lower.

1. Correlations of Central Barriers with Reactant Properties. A linear correlation between the experimental central barriers, $\Delta H^{\ddagger}_{cent}$, for reaction at carbon (eq 1) and the methyl cation affinities (MCAs) of X^- was previously noted.[23c,d,39] However, our G2(+) data for this reaction set indicated that such a correlation breaks down for X = F.[2] In the present study, we find, as for reaction at carbon, that the analogous linear correlation between the $\Delta H^{\ddagger}_{cent}$ values for reaction at nitrogen and amino cation affinities (ACAs)[40] also breaks down for X = F (data in Table 7). Similarly, $\Delta H^{\ddagger}_{cent}$ values for substitution at nitrogen do not correlate with X^- proton affinities; the correlation again breaks down for X = F, as was found for substitution at carbon.

In our recent study of halide substitution at carbon, we found a reasonable linear correlation between the central barriers and IE(X^-) values (R^2 = 0.857).[2] A similar correlation (R^2 = 0.896) is obtained for reaction at nitrogen (Figure 6) although, as for carbon, the significance of this correlation is not clear.

We previously found[2] that a correlation between the central S_N2 barriers, $\Delta H^{\ddagger}_{cent}$, at carbon and the D_{C-X} bond dissociation energies in CH_3X fails for X = F.[2] We find here that correlation of the central barriers at nitrogen with the D_{N-X} bond dissociation energies in NH_2X (listed in Table 8) also fails for X = F.

Table 7. Calculated G2(+) Amino Cation Affinities (ACA, kJ mol^{-1}) and Proton Affinities (PA, kJ mol^{-1}) of Halide Anions (X^-)

X	G2(+) ACA[a] (0 K)	G2(+) PA (0 K)	G2(+) PA (298 K)	exptl PA[b] (298 K)
F	1034.1	1546.8	1550.5	1554 ± 1
Cl	982.6	1394.7	1398.4	1395 ± 1
				1396 ± 9
Br	970.9	1351.2	1354.9	1354
				1349 ± 9
I	977.7	1314.1	1317.8	1315

[a] Energies of the reactions $NH_2X \rightarrow NH_2^+ (^3B_1) + X^-$. The lowest singlet ($^1A_1$) state of NH_2^+ lies 131.3 kJ mol^{-1} above the $^3B_1$ ground state at the G2(+) level (see ref 40). [b] Experimental data taken from ref 3.

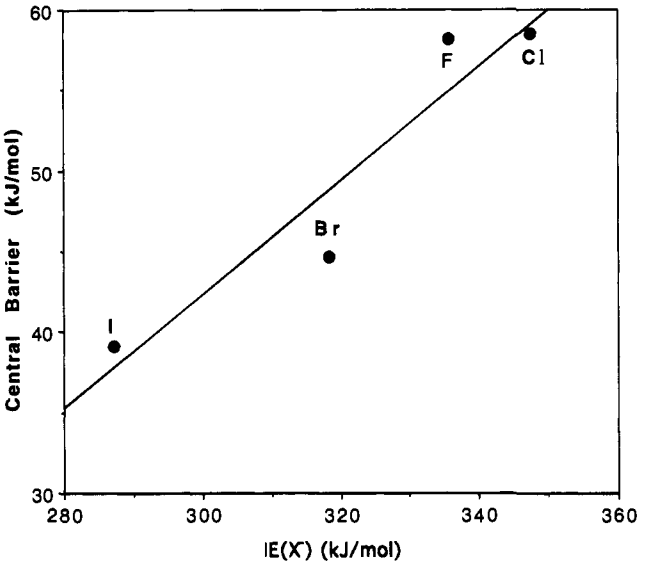

Figure 6. Plot of G2(+) central barriers ($\Delta H^{\ddagger}_{cent}$, 0 K) for substitution at nitrogen vs G2(+) gas-phase ionization energies of X^- (IE(X^-)). G2(+) values of IE(X^-) are taken from ref 2.

(39) Han, C.-C.; Dodd, J. A.; Brauman, J. I. *J. Phys. Chem.* **1986**, *90*, 471.

(40) Amino cation affinities for X^- are the energy changes for the reactions $NH_2X \rightarrow NH_2^+ (^3B_1) + X^-$. We find a singlet−triplet gap for NH_2^+ at the G2(+) level of 131.3 kJ mol^{-1}, in reasonable agreement with the experimental 125.9 kJ mol^{-1}.[41] There appears to be an error in a recent study[42] of NH_2^+, leading to an unrealistic singlet−triplet gap of 370.1 kJ mol^{-1} at the QCISD(T)/6-311+G(3df,2p)//MP2/6-31G(d,p) + ZPVE level.

(41) Gibson, S. T.; Greene, J. P.; Berkowitz, J. *J. Chem. Phys.* **1985**, *83*, 4319.

(42) Qi, F.; Sheng, L.; Zhang, Y.; Yu, S.; Li, W.-K. *Chem. Phys. Lett.* **1995**, *234*, 450.

Table 8. Calculated G2(+) Dissociation Energies (D_{N-X}, 0 K and D_{C-X}, 0 K) (X = F–I), Binding Energies of the Transition Structures (E_b(TS), 0 K), and the Thermochemical Looseness Index ($T^{\ddagger}$) for S_N2 Reactions at Nitrogen and at Carbon[a]

				E_b(TS)		$T^{\ddagger}$	
	D_{N-X}	D_{C-X}		at N	at C	at N,	at C
X =	G2(+)[b]	G2(+)[b]	expt[c]	G2(+)[d]	G2(+)	G2(+)[e]	G2(+)
F	292.0	463.0	465.4	347.7	471.0	1.19	1.02
Cl	252.3	347.3	342.0	261.6	335.7	1.04	0.97
Br	210.8	285.5	289.9	224.5	279.7	1.06	0.98
I	187.1	237.2	231.2	198.0	230.6	1.06	0.97

[a] All energies are given in kJ mol^{-1}. The $T^{\ddagger}$ values are dimensionless. [b] The G2(+) energies of $NH_2^{\bullet}$ and $CH_3^{\bullet}$ at 0 K are −55.788 96 and −39.744 95 hartrees, respectively. The G2(+)[ECP] energies of Br(^{2}P) and I(^{2}P) (−13.108 25 and −11.337 54 hartrees) were calculated with incorporation of spin–orbit corrections, see ref 19. [c] Calculated with the use of experimental $\Delta H_{f,0}$ data taken from ref 3. $\Delta H_{f,0}$ for CH_3F was calculated from the experimental $\Delta H_{f,298}$ using theoretical enthalpy temperature corrections (see ref 17n). [d] Defined by eq 6. [e] Defined by eq 5.

2. Correlations of Central Barriers with Energetic and Geometrical Characteristics of the Transition Structures. Earlier work[12a,43,44] has found that the loseness of S_N2 transition structures in the methyl-transfer reactions for a range of nucleophiles including fluoride and chloride anions correlates with the magnitude of the activation barrier. At the G2(+) level of theory, we reported a reasonable correlation between central barriers and the looseness of the MP2 transition structure geometries for all halogens ($R^2 = 0.939$).[2] For substitution at nitrogen a correlation of the central barrier with % N–X‡ is also found, though of poorer quality ($R^2 = 0.887$).

Thermochemical looseness of the transition structures **2a**–**2d** may be expressed by a thermochemical looseness index, $T^{\ddagger}$:

$$T^{\ddagger} = E_b(\mathrm{TS})/D_{N-X} \quad (5)$$

(analogous to that proposed[45] for substitution at carbon), where E_b(TS) is the binding energy of the transition structure and D_{N-X} is the N–X bond dissociation energy in NH_2X. As for carbon,[12a] the binding energy of the transition structure, E_b(TS), may be defined by

$$E_b(\mathrm{TS}) = E[\mathrm{XNH_2X^-}]^{\ddagger} - E(\mathrm{X^{\bullet}}) - E(\mathrm{NH_2^{\bullet}}) - E(\mathrm{X^-}) \quad (6)$$

While a correlation between the thermochemical index, $T^{\ddagger}$, and the geometrical index, % C–X‡, for the identity S_N2 reactions at carbon at the HF level has been noted by Shaik,[45] we found no such correlation at the G2(+) level.[2] In the present study of substitution at nitrogen, we also find that the analogous correlation between T‡ and % N–X‡ breaks down for X = F. Similarly, no correlation is found between the central barriers ($\Delta H^{\ddagger}_{cent}$) and T‡.

Conclusions

Application of G2(+) theory to the identity S_N2 exchange reaction of halide ion at saturated nitrogen (eq 2), and comparison of the results with the corresponding data for exchange at saturated carbon (eq 1), leads to the following conclusions:

(1) Central barrier heights ($\Delta H^{\ddagger}_{cent}$) for substitution at nitrogen for X = F=I are very similar in magnitude, spanning a range of just 19.4 kJ mol^{-1} (compared with 13.0 kJ mol^{-1} for the reaction at carbon). The barrier heights decrease in the following order: Cl (58.5 kJ mol^{-1}) ≥ F (58.2 kJ mol^{-1}) > Br (44.7 kJ mol^{-1}) > I (39.1 kJ mol^{-1}). For X = Br and I, the central barriers for nucleophilic substitution at nitrogen are slightly lower than those at saturated carbon, while for X = F and Cl the central barriers are slightly higher. Thus, our data indicate that (i) the barriers for identity exchange reactions of the set of halide ions are similar in magnitude despite the wide range in the N–X and C–X bond strengths and in the proton affinities of X$^-$ and (ii) the barrier heights are not greatly affected by the identity of the central atom, C or N.

(2) Overall barriers ($\Delta H^{\ddagger}_{ovr}$) for substitution at nitrogen are *negative* for all halogens, while in the case of the analogous reactions at saturated carbon, this barrier is negative only for X = F. The lower barriers are consistent with the greater complexation energies calculated for the X$^-$···HNHX systems. Our results suggest that nucleophilic substitution at nitrogen is likely to be a relatively facile process in the gas phase, and to take place more readily than at carbon.

(3) Central barriers ($\Delta H^{\ddagger}_{cent}$) do not appear to correlate with the amino cation affinities of X$^-$ (ACA(X$^-$)) nor with the proton affinities of X$^-$ (PA(X$^-$)), nor with the binding energies of the transition structures, E_b(TS). This lack of correlation was also observed for the corresponding reactions at carbon. However, a reasonable correlation is found between $\Delta H^{\ddagger}_{cent}$ and IE(X$^-$) values for substitution at nitrogen (as was found in the reactions at carbon).

(4) Complexation energies (ΔH_{comp}) of the ion–molecule complexes X$^-$···HNHX (**1**) are found to decrease in the following order: F (114.0 kJ mol^{-1}) > Cl (67.8 kJ mol^{-1}) > Br (58.4 kJ mol^{-1}) > I (50.0 kJ mol^{-1}). These complexation energies are larger than those found for the corresponding carbon complexes, consistent with the effective hydrogen-bonding ability of N–H bonds. Complexation energies of the X$^-$···HNHX complexes are found to correlate with halogen electronegativity.

(5) G2(+) central barriers, $\Delta H^{\ddagger}_{cent}$, for substitution at nitrogen correlate with the geometrical looseness (% N–X‡) of the transition structures **2**, but not with the thermochemical looseness parameter ($T^{\ddagger}$). These results also parallel those found for substitution at carbon.

(6) Comparison of our computational data with earlier lower level calculations reaffirms that both the high level of electron correlation and the large basis sets employed in G2(+) theory are important in obtaining reliable barrier heights for nucleophilic substitution reactions.

Acknowledgment. We gratefully acknowledge a generous allocation of time on the Fujitsu VP-2200 computer of the Australian National University Supercomputer Facility, the support of the Australian Research Council, and the award (to A.P.) of an ARC Senior Research Fellowship.

Supporting Information Available: NPA charge distributions for NH_2X (Table S1), X$^-$···H_2NX ion–molecule complexes (**1**) and transition structures (**3**) (Table S2), and C_{2v} XNH_2X^- transition structures (**2**) Table S3 (X = F, Cl, Br, and I) (3 pages). This material is contained in many libraries on microfiche, immediately follows this article in the microfilm version of the journal, can be ordered from the ACS, and can be downloaded from the Internet; see any surrent masthead page for ordering information and Internet access instructions.

JA9504404

(43) Shaik, S. S.; Schlegel, H. B.; Wolfe, S. *J. Chem. Soc., Chem. Commun.* **1988**, 1322.
(44) Wolfe, S.; Kim, C.-K. *J. Am. Chem. Soc.* **1991**, *113*, 8056.
(45) Shaik, S. S. *J. Am. Chem. Soc.* **1988**, *110*, 1127.